

**High temperature phase transitions in synthetic  
RbGaSi<sub>2</sub>O<sub>6</sub> and RbFeSi<sub>2</sub>O<sub>6</sub> leucite analogues**

BELL, Anthony <<http://orcid.org/0000-0001-5038-5621>>

Available from Sheffield Hallam University Research Archive (SHURA) at:

<http://shura.shu.ac.uk/32985/>

---

This document is the author deposited version. You are advised to consult the publisher's version if you wish to cite from it.

**Published version**

BELL, Anthony (2022). High temperature phase transitions in synthetic RbGaSi<sub>2</sub>O<sub>6</sub> and RbFeSi<sub>2</sub>O<sub>6</sub> leucite analogues. In: British Crystallographic Association Spring Meeting, Leeds, UK, 11-14 Apr 2022. British Crystallographic Association. (Unpublished)

---

**Copyright and re-use policy**

See <http://shura.shu.ac.uk/information.html>

# High temperature phase transitions in synthetic RbGaSi<sub>2</sub>O<sub>6</sub> and RbFeSi<sub>2</sub>O<sub>6</sub> leucite analogues.

**Sheffield Hallam University** | Materials and Engineering Research Institute

**A.M.T.Bell (Anthony.Bell@shu.ac.uk)**

## Introduction

Leucite (KAISi<sub>2</sub>O<sub>6</sub>) [1] is a tetrahedrally coordinated silicate framework mineral. Synthetic analogues of leucite can be synthesised with stoichiometries of A<sup>2+</sup>B<sup>2+</sup>Si<sub>5</sub>O<sub>12</sub> or A<sup>+</sup>C<sup>3+</sup>Si<sub>2</sub>O<sub>6</sub>, with some of the silicon framework cations partially replaced by divalent (B) or trivalent (C) cations. A monovalent extraframework alkali metal (A) cation is also incorporated in these structures to balance the charges. Ambient temperature structures of synthetic anhydrous leucite analogues (where A = K or Rb and C = Al, Ga or Fe) all have I<sub>4</sub>/a tetragonal structures [1-5] with **disordered** tetrahedrally coordinated sites (T-sites).

On heating these tetragonal leucites can undergo phase transitions to I<sub>a</sub>-3d cubic. Phase transitions have been reported for KCSi<sub>2</sub>O<sub>6</sub> [2, 4] and RbAlSi<sub>2</sub>O<sub>6</sub> [4]. High temperature X-ray powder diffraction has been done on RbGaSi<sub>2</sub>O<sub>6</sub> and RbFeSi<sub>2</sub>O<sub>6</sub> leucite analogues to look for more phase transitions.

## Synthesis

RbGaSi<sub>2</sub>O<sub>6</sub> and RbFeSi<sub>2</sub>O<sub>6</sub> were prepared from appropriate stoichiometric mixtures of Rb<sub>2</sub>CO<sub>3</sub>, SiO<sub>2</sub>, and Ga<sub>2</sub>O<sub>3</sub> or Fe<sub>2</sub>O<sub>3</sub>, each mixture was loaded into Pt crucibles. The RbGaSi<sub>2</sub>O<sub>6</sub> mixture was heated to 1473K and the RbFeSi<sub>2</sub>O<sub>6</sub> mixture was heated to 1673K.

## Data collection and analysis

Each sample was loaded into a Pt flat plate sample holder which was inserted in an Anton Paar HTK1200N high temperature stage mounted on a PANalytical X'Pert Pro MPD. High temperature X-ray powder diffraction data, using Cu K $\alpha$  X-rays and a PIXCEL-1D area detector, were collected on RbGaSi<sub>2</sub>O<sub>6</sub> up to 973K and on RbFeSi<sub>2</sub>O<sub>6</sub> up to 873K.

The I<sub>4</sub>/a tetragonal structure for RbGaSi<sub>2</sub>O<sub>6</sub> [5] was used as a starting model for Rietveld refinement, Ga<sub>2</sub>O<sub>3</sub> impurity [6] was included as a second phase for Rietveld refinements [7] which were done using FULLPROF [8].

The I<sub>4</sub>/a tetragonal structure for RbFeSi<sub>2</sub>O<sub>6</sub> [4] was used as a starting model for Rietveld refinement. Mössbauer Spectroscopy [9] on the RbFeSi<sub>2</sub>O<sub>6</sub> sample also showed the presence of Fe<sub>3</sub>O<sub>4</sub> [10], so this was included as a second phase for Rietveld refinements which were done using GSAS-II [11].

## High temperature X-ray Powder Diffraction.

Figure 1 (RbGaSi<sub>2</sub>O<sub>6</sub>) and Figure 2 (RbFeSi<sub>2</sub>O<sub>6</sub>) show how the tetragonal 004 and 400 Bragg reflections converge to a single cubic 400 reflection on heating. Rietveld refinements below the transition were done using the ambient temperature I<sub>4</sub>/a tetragonal structures. Above the transition Rietveld refinements were done using the I<sub>a</sub>-3d cubic structures for CsGaSi<sub>2</sub>O<sub>6</sub> [5] and CsFeSi<sub>2</sub>O<sub>6</sub> [3] as starting structures with Rb replacing Cs. Figure 1 shows that the RbGaSi<sub>2</sub>O<sub>6</sub> transition takes place at 733K and Figure 2 shows that the RbFeSi<sub>2</sub>O<sub>6</sub> transition takes place at 673K. Figure 3 shows how the lattice parameters change with temperature for both RbGaSi<sub>2</sub>O<sub>6</sub> and RbFeSi<sub>2</sub>O<sub>6</sub>. Figures 4 and 5 show the Rietveld difference plots for RbFeSi<sub>2</sub>O<sub>6</sub> at 603K and 773K. Figures 6 and 7 show VESTA [12] plots of crystal structures for RbFeSi<sub>2</sub>O<sub>6</sub> at 603K and 773K, pink spheres represent Rb<sup>+</sup> cations, blue tetrahedra represent disordered (Si,Fe)O<sub>4</sub> units and red spheres represent O<sup>2-</sup> anions.

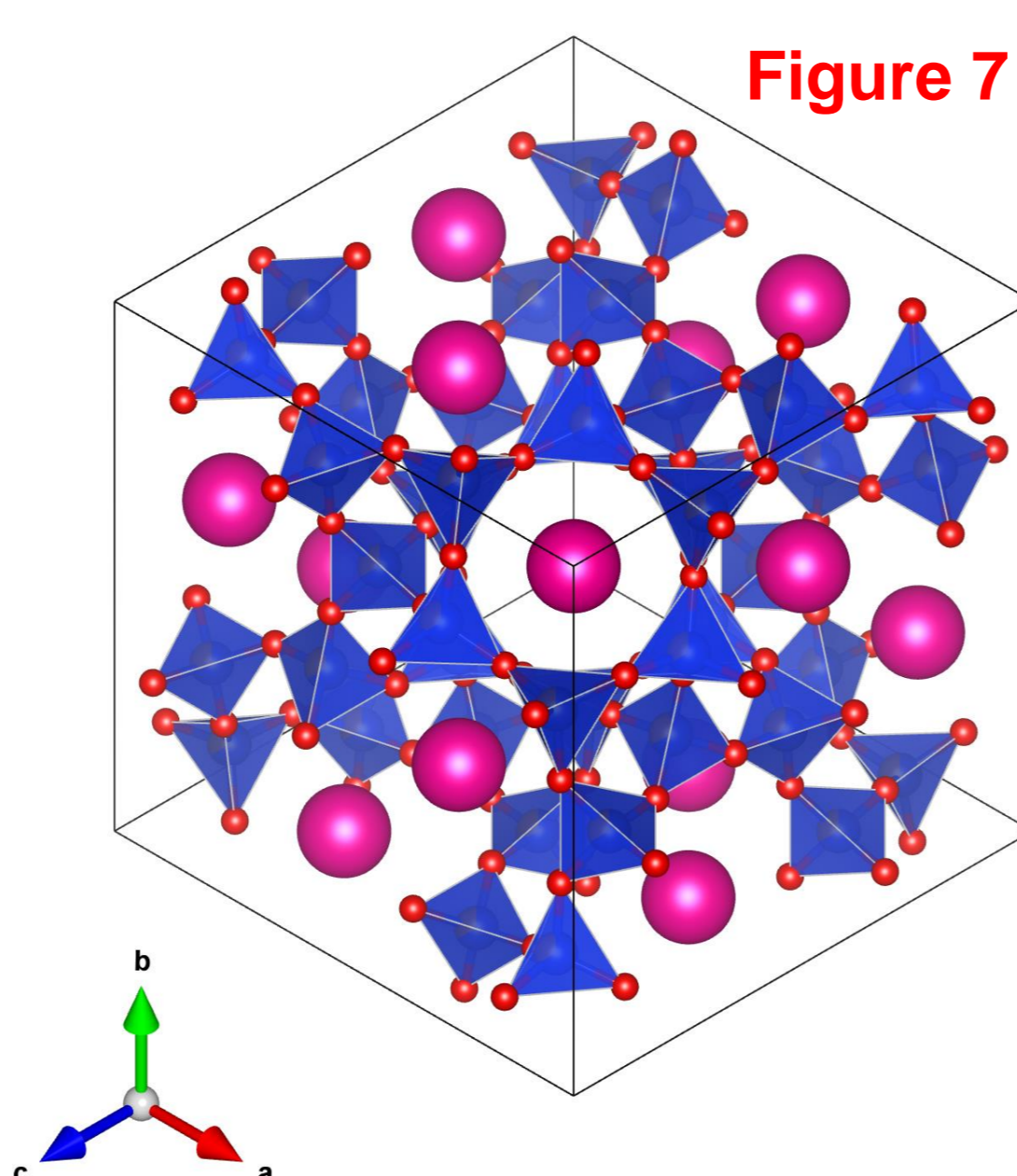
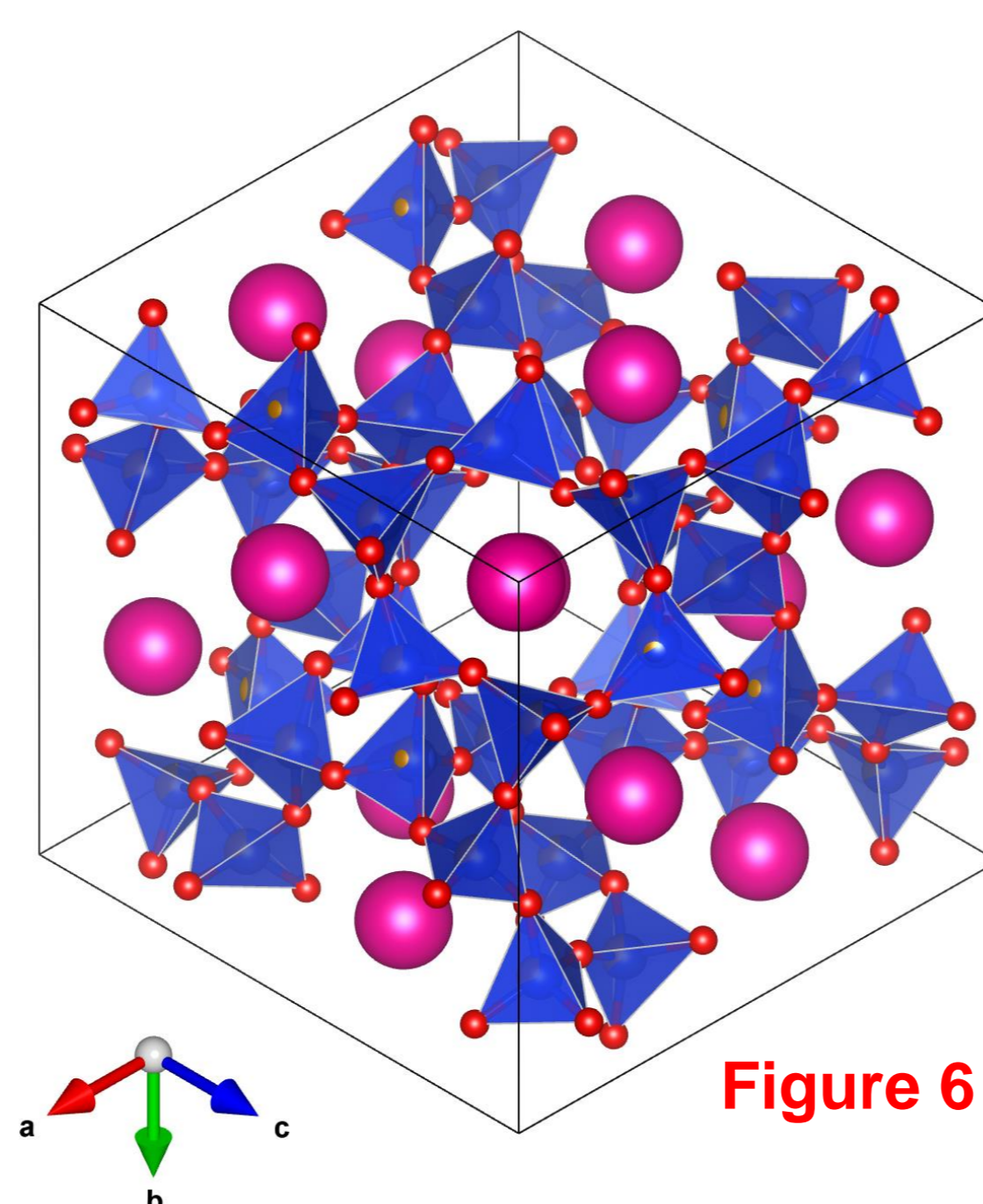
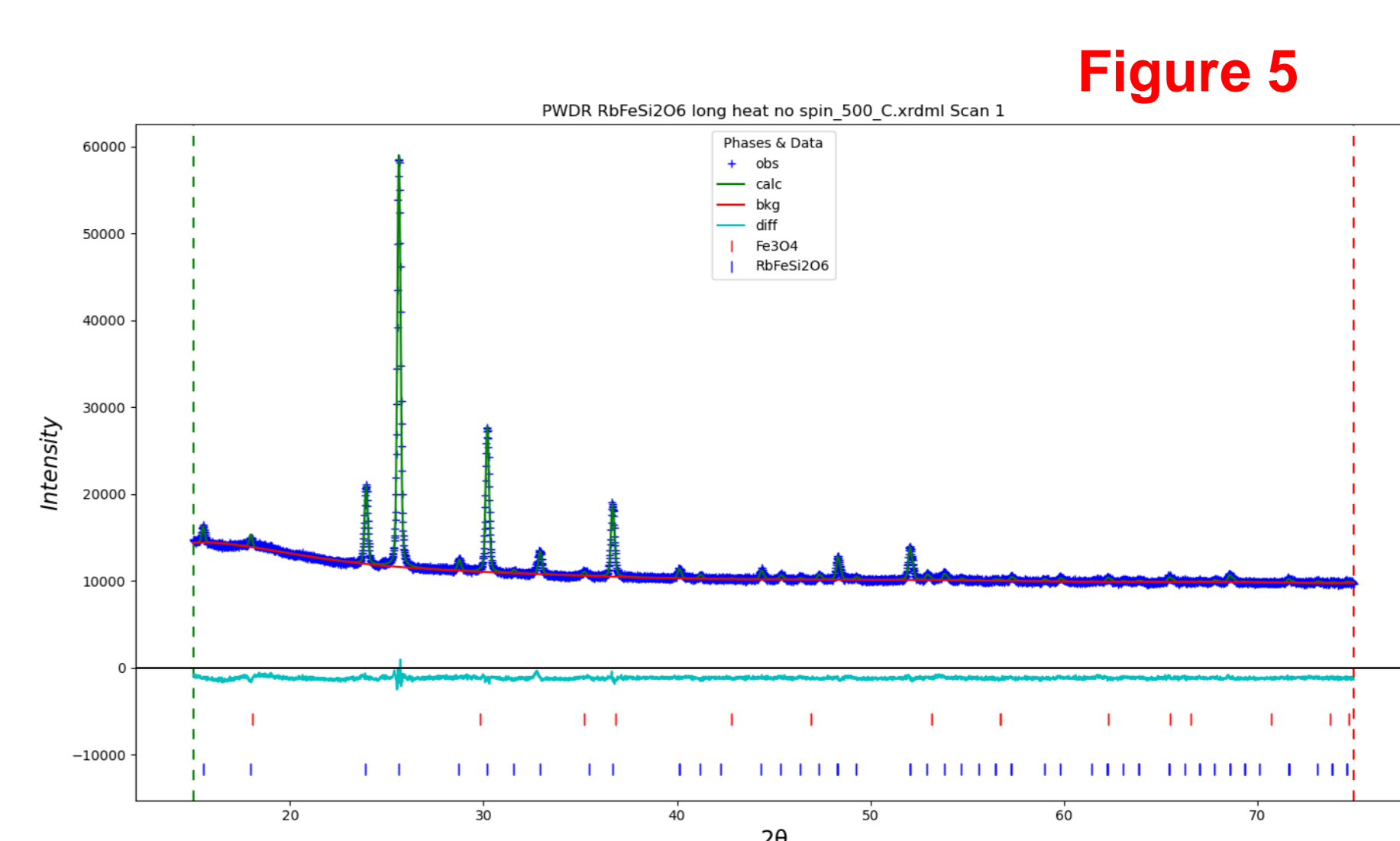
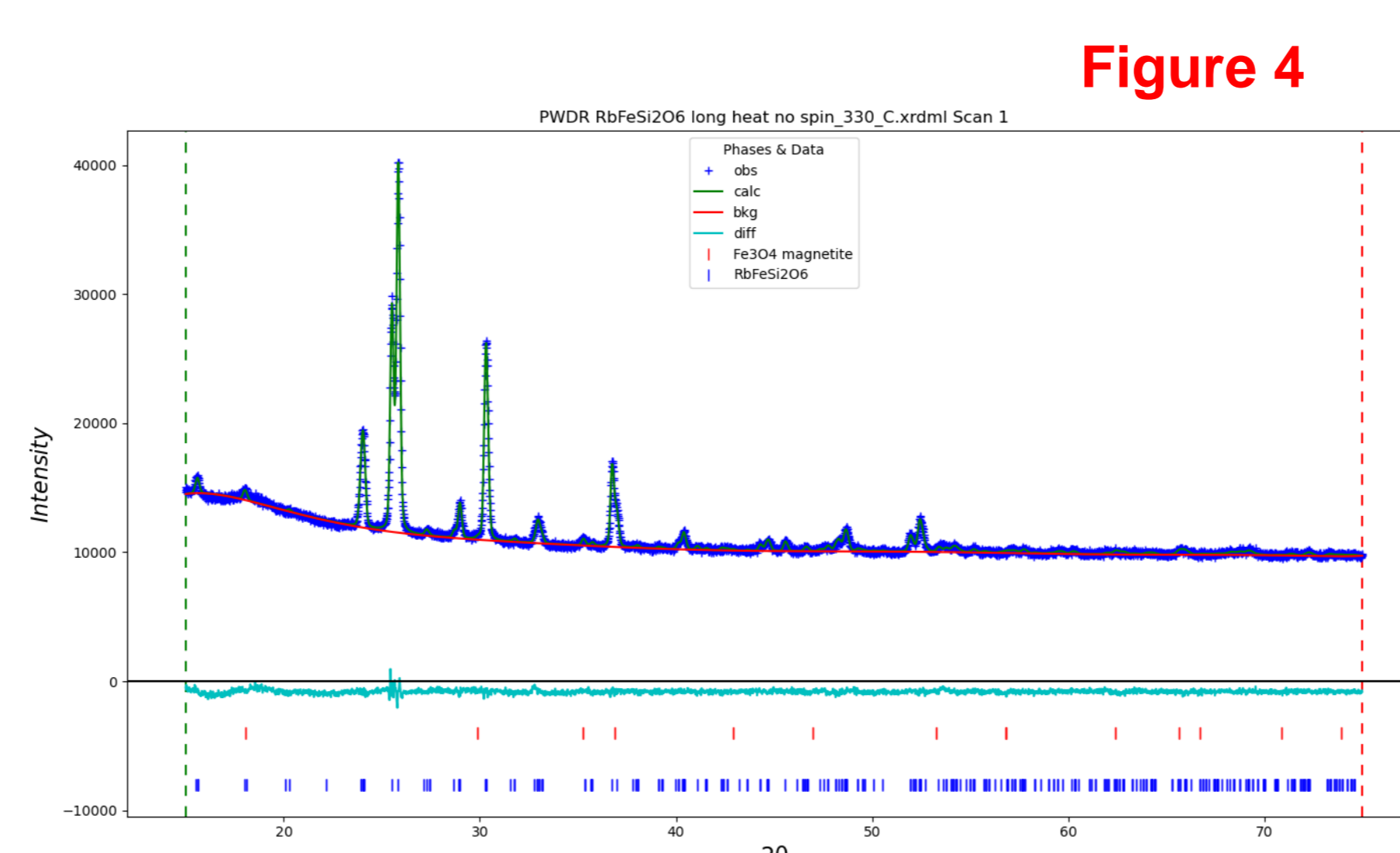
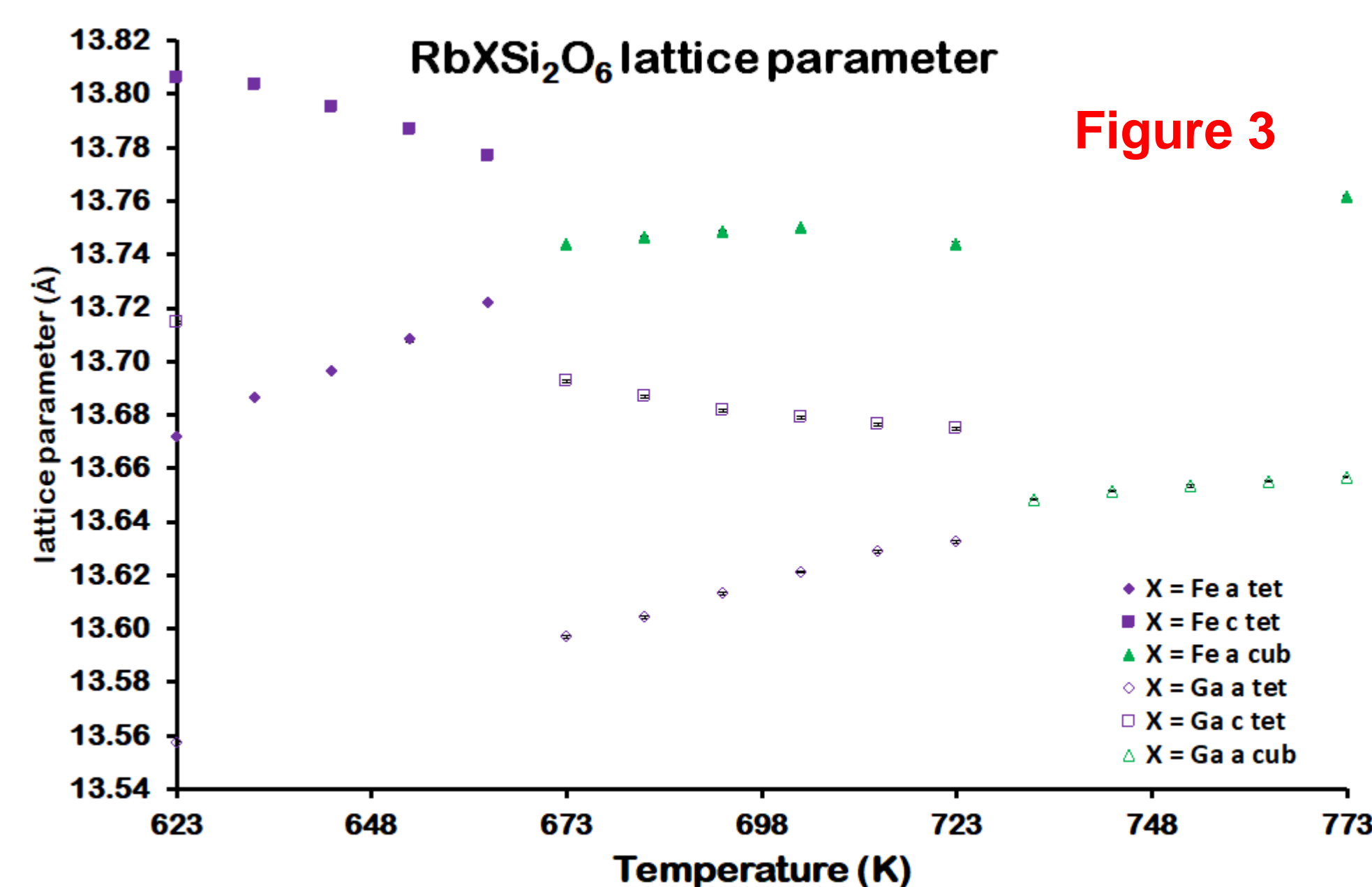
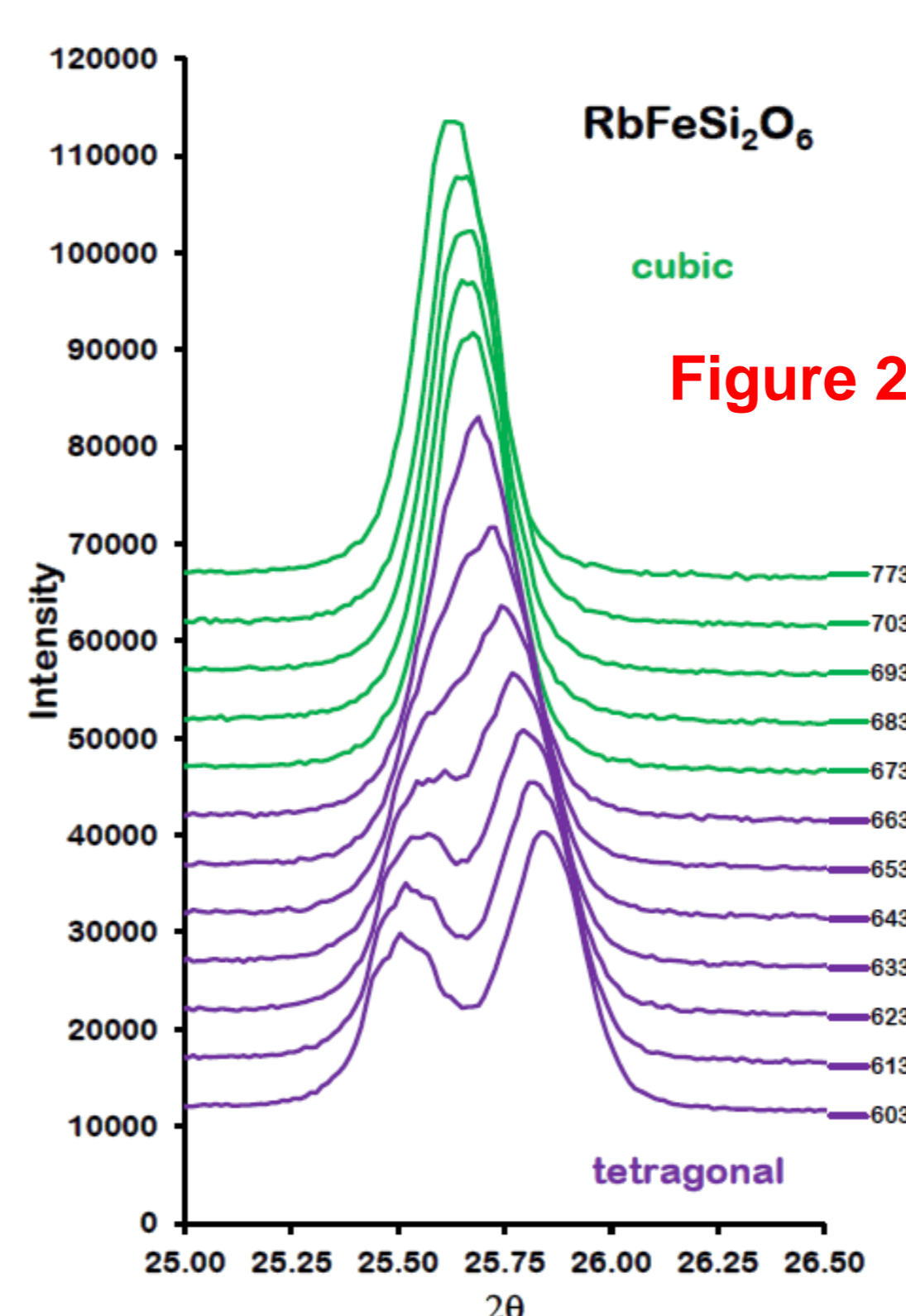
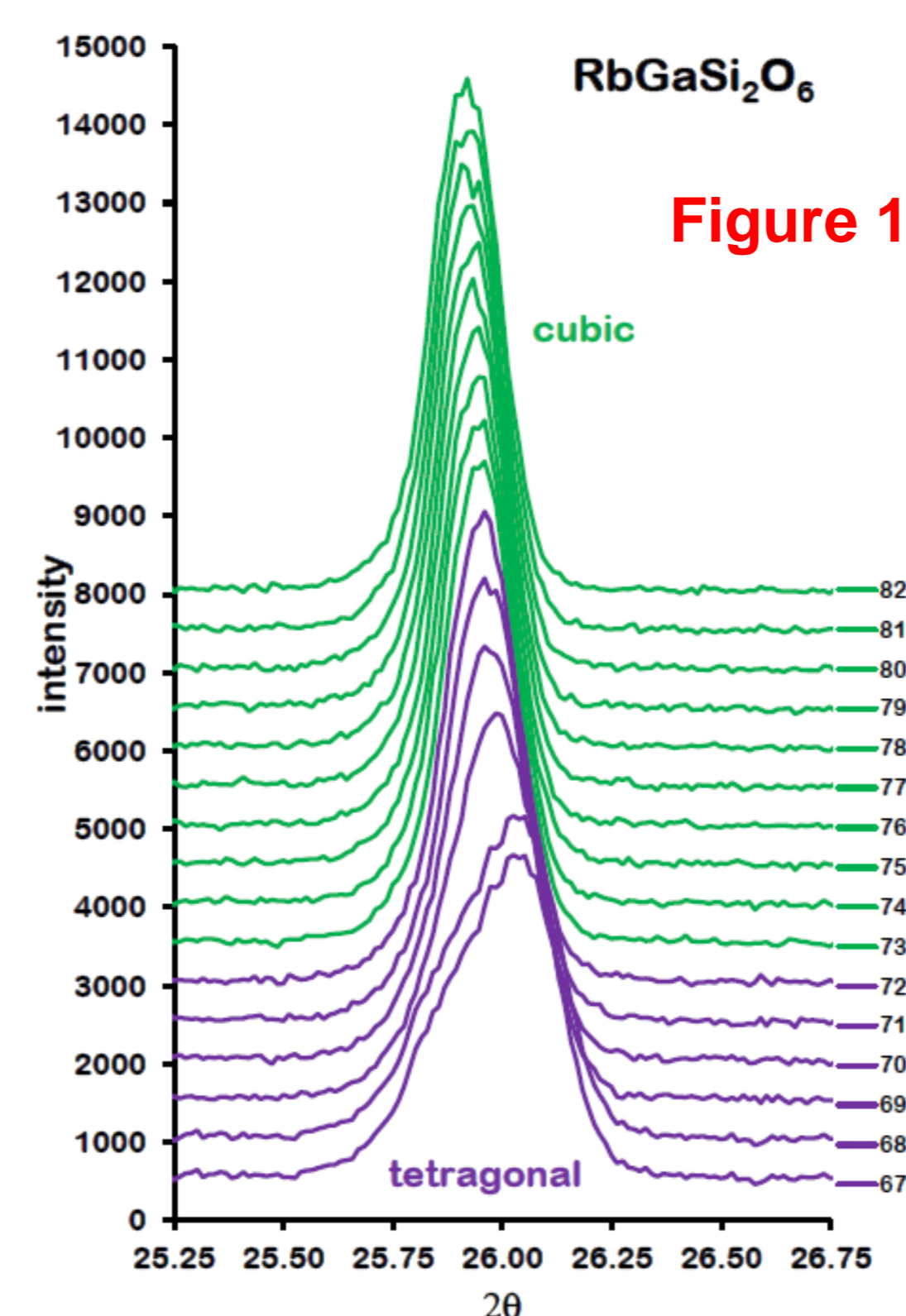


**Table 1 - Ambient temperature lattice parameters and I<sub>4</sub>/a tetragonal to I<sub>a</sub>-3d cubic phase transition temperatures (T) for A<sup>+</sup>C<sup>3+</sup>Si<sub>2</sub>O<sub>6</sub> leucite analogues.**

Stoichiometry	a(Å)	c(Å)	c/a	T (K)	Reference
KAISi <sub>2</sub> O <sub>6</sub>	13.0548(2)	13.7518(2)	1.05339(3)	943	[4]
KGaSi <sub>2</sub> O <sub>6</sub>	13.1099(4)	13.8100(4)	1.05340(6)	773-973	[2]
KFeSi <sub>2</sub> O <sub>6</sub>	13.2036(2)	13.9545(3)	1.05687(4)	853	[4]
RbAlSi <sub>2</sub> O <sub>6</sub>	13.2918(2)	13.7412(2)	1.03381(3)	753	[4]
RbGaSi <sub>2</sub> O <sub>6</sub>	13.3752(6)	13.8040(6)	1.03206(9)	733	This work
RbFeSi <sub>2</sub> O <sub>6</sub>	13.4500(15)	13.9274(7)	1.03549(17)	673	This work

## Discussion

High temperature X-ray powder diffraction has been done on RbGaSi<sub>2</sub>O<sub>6</sub> and RbFeSi<sub>2</sub>O<sub>6</sub> leucite analogues, in both cases there are phase transitions from I<sub>4</sub>/a tetragonal to I<sub>a</sub>-3d cubic. Ambient temperature lattice parameters and transition temperatures are given in Table 1 for 6 different A<sup>+</sup>C<sup>3+</sup>Si<sub>2</sub>O<sub>6</sub> leucite analogues. Figures 6 (I<sub>4</sub>/a 603K) and 7 (I<sub>a</sub>-3d 773K) show crystal structures for RbFeSi<sub>2</sub>O<sub>6</sub>. Note how the tetragonal framework is more collapsed [13] than the cubic framework.

Due to the smaller ionic radii [14] for K<sup>+</sup> compared to Rb<sup>+</sup> the KCSi<sub>2</sub>O<sub>6</sub> leucite analogues have higher c/a ratios and transition temperatures than the corresponding RbCSi<sub>2</sub>O<sub>6</sub> leucite analogues. The smaller alkali metal cation ionic radius for K<sup>+</sup> compared to Rb<sup>+</sup> means a greater framework collapse. Consequently more energy is needed to expand the framework to a less collapsed cubic structure increasing the transition temperature.

## Conclusions

High temperature X-ray powder diffraction has been done on RbGaSi<sub>2</sub>O<sub>6</sub> and RbFeSi<sub>2</sub>O<sub>6</sub> leucite analogues. In both cases there are I<sub>4</sub>/a tetragonal to I<sub>a</sub>-3d cubic phase transitions. The transition temperatures are 733K (RbGaSi<sub>2</sub>O<sub>6</sub>) and 673K (RbFeSi<sub>2</sub>O<sub>6</sub>).

**References:-** [1] Mazzi, F., *et al.* (1976). *Am. Mineral.*, 61, 108-115. [2] Bell, A.M.T. & Henderson, C.M.B. (2020). *Journal of Solid State Chemistry*, 284, 121142. [3] Bell, A.M.T. & Henderson, C.M.B. (1994). *Acta Cryst.*, C50, 1531-1536. [4] Palmer, D.C., *et al.* (1997). *Am. Mineral.*, 82, 16-29. [5] Bell, A.M.T. & Stone A.H. (2021). *Powder Diffraction*, 36(4), 273-281. [6] da Silva, M. A. F. M., *et al.* (2012). *Journal of Physics: Conference Series* 340, 1-7. [7] Rietveld, H. M. (1969). *J. Appl. Cryst.* 2, 65-71. [8] Rodríguez-Carvajal, J. (1993). *Phys. B: Condens. Matter*, 192, 55-69. [9] Bell, A.M.T. & Scrimshire A. (2021). *In preparation*. [10] Fleet, M. E. (1981). *Acta Cryst.* B37, 917-920. [11] Toby B.H. & Von Dreele R.B. (2013). *J. Appl. Cryst.* 46, 544-549. [12] Momma, K. & Izumi, F. (2008). *J. Appl. Cryst.* 41, 653-658. [13] Taylor, D. & Henderson, C.M.B. (1968). *Am. Mineral.*, 53, 1476-1489. [14] Shannon, R. D. (1976). *Acta Cryst.* A32, 751-767.